Published in final edited form as:
J Parasitol. 2004 October ; 90(5): 980–990.

MICROBIAL ADHESION OF *CRYPTOSPORIDIUM PARVUM* SPOROZOITES: PURIFICATION OF AN INHIBITORY LIPID FROM BOVINE MUCOSA

Julie K. Johnson[*], **Joann Schmidt**, **Howard B. Gelberg**[†], and **Mark S. Kuhlenschmidt**
Department of Pathobiology, College of Veterinary Medicine, University of Illinois at Urbana-Champaign, 2001 South Lincoln Avenue, Urbana, Illinois 61802. e-mail: kuhlensc@uiuc.edu

Abstract

Cryptosporidium parvum is a protozoan pathogen of humans and livestock worldwide. Its ability to infect a wide range of species raises questions as to the involvement of a specific host cell receptor for parasite–host recognition. To investigate the mechanism of parasite–host cell recognition, we have developed an in vitro cell suspension binding assay to investigate adhesion of *C. parvum* sporozoites to host cells. Morphologic features of binding events observed with this assay were identical to those described in natural infections. Glycoconjugates, Madin Darby bovine kidney (MDBK) cell fractions, and plasma membrane vesicles (PMVs) were screened for their ability to block binding of sporozoites to MDBK cells. Mucins, MDBK cell fractions, and PMVs exhibited dose-dependent inhibition of sporozoite binding. The major inhibitory fraction from MDBK cells was found to be insoluble in aqueous medium, nonsaponifiable, and lacking carbohydrate moieties, nitrogen, and phosphorus. Its inhibitory effect was resistant to heat, protease digestion, and glycosidase treatment, suggesting that the inhibitory activity is a lipid or a lipid-like component. The inhibitory activity was purified from MDBK cells, and in larger amounts from bovine small intestinal mucosa, by organic solvent extraction, semipreparative high-pressure liquid chromatography, and preparative high-performance thin-layer chromatography. Biochemical analyses, thin-layer chromatography staining techniques, mass spectrometry, and elemental analysis were used to partially characterize the purified lipid. These results indicate that a host intestinal lipid(s) or a lipid-like component(s) may play an important role in the early stages of host cell invasion by *C. parvum*.

Cryptosporidium parvum is a common cause of diarrhea in the young and the immunocompromised (Fayer, 1990; Fayer et al., 1997). Infection with this apicomplexan parasite usually results in acute, self-limiting diarrhea in immunocompetent hosts (Current et al., 1983; Wolfson et al., 1985). In immunocompromised hosts, such as acquired immune deficiency syndrome patients, infection may lead to severe and life-threatening diarrhea. *Cryptosporidium parvum* was responsible for the largest outbreak of waterborne disease in U.S. history in Milwaukee, Wisconsin, resulting in the infection of approximately 403,000 people and demonstrating the great epidemic potential of this organism (MacKenzie et al., 1994). It has become the most important contaminant found in drinking water and is now recognized as a significant public health concern. Unfortunately, *C. parvum* is both ubiquitous and difficult to remove from water supplies (Rose et al., 1997).

Correspondence to: Mark S. Kuhlenschmidt.
[*]Present address: 3M Corporate Headquarters, 3M Center, St. Paul, Minnesota 55144-1000.
[†]Present address: College of Veterinary Medicine, Oregon State University, Corvallis, Oregon 97331.

Most traditional chemotherapeutic agents that are effective against other apicomplexans target the intracellular forms of the parasites. To date, this approach has not been successful in treating cryptosporidiosis (Tzipori and Ward, 2002). Collectively, these findings strongly support the concept that an additional approach to the prevention and treatment of *C. parvum* infection is warranted. Our approach has been to focus on the initial recognition and adhesion events between *C. parvum* sporozoites and host cells. Our goal has been the elucidation of mechanisms responsible for parasite–host cell recognition.

Cryptosporidium parvum sporozoite binding to host cells in vitro is highly labile. After excystation, sporozoites rapidly lose their ability to bind host cells during both static and rotation incubations at 37 C. Interestingly, this loss of binding activity is not explained by a comparable loss in viability. Sporozoites also do not adhere to host cells at 4 C. Such biological constraints of sporozoite-binding activity present a challenge to the development of traditional in vitro biochemical assays to quantify microbial adhesion kinetics of *C. parvum* sporozoites. In numerous attempts to develop this type of assay, we discovered that any postexcystation procedure designed to fluorescently or radioactively label freshly excysted sporozoites, especially if performed at 37 C, markedly reduced the sporozoite's ability to bind host cells (J. K. Johnson et al., unpubl.).

These observations led us to conclude that a cell suspension assay that rapidly measures biologically relevant adhesion events between sporozoites and host cells is essential for studying the mechanisms of adhesion as it likely occurs in vivo. Previously developed attachment assays (Hamer et al., 1994; Chen and LaRusso, 2000) used cell monolayers and involved fixing the cells before exposure to sporozoites to prevent invasion. After incubation with sporozoites, the cells were removed from the monolayers, and the number of bound sporozoites was determined by microscopy. Although these assays measured sporozoite attachment, they used fixed cells, which may or may not reflect adhesive mechanisms occurring in vivo. In addition, the numerous steps involved in fixing and processing these monolayer cells were not amenable to our goal of rapidly measuring early, in vivo–relevant adhesion events. Accordingly, we report in this study the development of an in vivo–simulating sporozoite-binding assay that measures physiologically relevant sporozoite adhesion to host cells during gentle end-over-end rotation in suspension. Under these conditions, which attempt to approximate the shear forces generated by peristalsis in the host gut, we can rapidly quantify the kinetics of adhesion of sporozoites to host cells and screen the ability of potential receptors, receptor mimics, or other compounds to inhibit this interaction. This assay measures initial host–parasite recognition events, allowing investigation of a complex, dynamic system that may involve multiple host and sporozoite receptors. We have used this assay to isolate and partially characterize a lipid molecule from calf intestinal mucosa that dose-dependently inhibits sporozoite adhesion. As such, it serves as a candidate for further exploration as a potential therapeutic agent.

MATERIALS AND METHODS

Materials

Unless stated otherwise, all reagents and chemicals were obtained from Sigma (St. Louis, Missouri) and were of the highest purity available. Globosides were obtained from Matreya Inc. (Pleasant Gap, Pennsylvania). All solvents were Burdick & Jackson high-pressure liquid chromatography (HPLC) grade obtained from Fisher Scientific (Hanover Park, Illinois). Thin-layer chromatography (TLC) and high-performance thin-layer chromatography (HPTLC) plates were E. Merck Kieselgel 60 plates without fluorescent indicator obtained from VWR Scientific (West Chester, Pennsylvania).

Propagation and purification of oocysts

The AUCP-1 isolate of *C. parvum* was maintained by repeated passage in male Holstein calves (IACUC protocol #04070). Oocysts were purified from collected feces by sequential sieve filtration, Sheather's sugar floatation, and discontinuous cesium chloride density centrifugation using minor modifications of previously established protocols (Current, 1990). The final, purified oocysts were washed by centrifugation in Tris–ethylenediamine-tetraacetic acid (Tris-EDTA) buffer (50 mM Tris, 10 mM EDTA) and stored at 4 C in a solution of 50% Hanks' balanced salt solution (HBSS, GIBCO, Grand Island, New York) and 50% antibiotic–antimycotic solution consisting of 6 g penicillin, 10 g streptomycin, 25 mg amphotericin, and 8.5 g NaCl/L of water.

Excystation and purification of sporozoites

Sporozoites were excysted and filtration purified by modifications of a previously described procedure (Zopf and Roth, 1996). Briefly, purified oocysts were washed twice in HBSS by centrifugation at 1,500 *g* for 15 min, resuspended in HBSS, and treated with an equal volume of 40% (v/v) commercial laundry bleach (5.25% sodium hypochlorite) for 10 min before excystation. Oocysts were then washed 4 times with HBSS to remove the bleach. Oocysts suspended in HBSS were placed in a 37 C water bath for 60 min and then mixed with an equal volume of prewarmed excystation fluid consisting of 1.5% (wt/v in HBSS) sodium taurocholate and 0.5% (wt/v in HBSS) trypsin. After excystation for 45–60 min at 37 C, sporozoites were washed free of excystation fluid by centrifugation at 1,000 *g* for 10 min. Sporozoites were then separated from unexcysted oocysts and oocyst shells by sequential passage through 5- and 2-μM Nucleopore polycarbonate filters. Purified sporozoites were washed twice with ice-cold minimal essential medium (MEM), resuspended in ice-cold MEM, enumerated using a hemocytometer, and used in binding assays within 4 hr after isolation.

Host cells

Madin Darby bovine kidney (MDBK) cells were used as the routine host cell line and were obtained from the American Type Culture Collection (ATCC) (CCL 22, Rockville, Maryland) and cultured in MEM with 10% horse serum. Single-cell suspensions were obtained by harvesting flasks of confluent cells with 0.05% trypsin in 0.53-mM EDTA. In addition to MDBK cells, the following cell types were also obtained: Caco-2 (human colonic carcinoma), HT-29 (human colonic carcinoma), MA-104 (embryonic African green monkey kidney), human foreskin fibroblasts, murine neuroblastoma, adult canine erythrocytes, and neonatal bovine erythrocytes. Caco-2 cells were obtained from the ATCC and maintained in complete culture medium consisting of MEM with 20% fetal bovine serum. HT-29 cells were also maintained in MEM with 20% fetal bovine serum. MA-104 cells were maintained in MEM with 10% calf serum (Rolsma et al., 1994). Adult canine and neonatal bovine erythrocytes (originating from whole-blood samples) were obtained from the University of Illinois Veterinary Medicine Teaching Hospital (Urbana, Illinois). Tissue culture cells were trypsinized, washed once by centrifugation, and suspended in MEM without serum. They were enumerated by hemocytometer by trypan blue exclusion. Erythrocytes from whole blood were adjusted to an appropriate concentration and enumerated by hemocytometer.

For isolation of bovine enterocytes, a 5-day-old male Holstein calf was obtained from the University of Illinois Dairy and killed by intravenous injection of barbiturate. The small intestine was excised and rinsed thoroughly with chilled phosphate-buffered saline (PBS). The intestine was opened, and the mucosa was removed by gently scraping with a glass microscope slide. Approximately 1 ml of freshly scraped intestinal mucosa was placed in a plastic petri dish and minced with a razor blade in a small volume of cold digestion media containing 130 mM NaCl, 12 mM *N*-2-hydroxythylpiperazine-*N*′-2-ethane-sulfonic acid (HEPES), 3 mM NaH_2PO_4, 3 mM Na_2HPO_4, 3 mM KH_2PO_4, 2 mM $MgSO_4$, 1 mM $CaCl_2$, 0.01 mg/ml phenol

red, 10 mM glucose, and 1 mg/ml bovine serum albumin (BSA) in water (pH 7.3). The mucosa was then placed in a 50-ml polypropylene centrifuge tube, and the tube was filled with digestion media. The mucosa was washed once by centrifugation at 180 *g* for 5 min at 4 C. The pelleted mucosa was resuspended in 45 ml of warm digestion media containing 0.05% Pronase (crude protease, Type I from bovine pancreas) and incubated at 37 C for 20 min. The digestion media containing Pronase was removed by centrifugation, and the mucosal pellet was washed thrice with digestion media. The mucosa was then resuspended in 45 ml of warm digestion media containing 0.10% collagenase (Type IA from *Clostridium hemolyticum*) and incubated at 37 C for 20 min. Individualization of enterocytes was monitored microscopically. The digestion media containing collagenase was removed by centrifugation, and the mucosal pellet was washed 4 times with digestion media. The final mucosal pellet was suspended in a small volume of digestion media and stored on ice. Individualized enterocytes were enumerated using a hemocytometer.

Binding assays

Cryptosporidium parvum sporozoites and individualized host cells were incubated in suspension in MEM (without serum) in the presence or absence of various additives (host cell extracts, MDBK cell plasma membrane vesicles [PMVs], or defined glycoconjugates, see below) in a 1.5-ml conical microfuge tube. The sporozoite to cell ratio was 10:1, with 5×10^6 sporozoites and 5×10^5 host cells suspended in each tube in the presence or absence of the various additives, in a final incubation volume of 300 μl. The sporozoites and host cells were rotated end-over-end for 20 min at 8 rpm at 37 C. After incubation, 20-μl aliquots of the suspension volume were examined by phase contrast microscopy. Binding of the sporozoites to host cells was quantified as the number of binding events per 100 host cells. This assay was also used to screen various additives including glycoconjugates, MDBK cell homogenates, PMVs, and fractionated PMVs for their ability to competitively inhibit sporozoite binding to host cells. This competitive binding assay was conducted as described above except that host cells and sporozoites were placed in microfuge tubes containing various concentrations of test inhibitors. Inhibitory activity was determined for each additive by comparison with separate control incubations containing only host cells and sporozoites. All glycoconjugates were dried in 1.5-ml microfuge tubes and then dissolved in 100-μl MEM by sonication in a water bath sonicator. Glycoconjugates, except for the mucins and neoglycoproteins, were added in binding assays to a final concentration of 1–3 mg/ml. Mucins were added at a concentration of 0.05 mg/ml. The neoglycoproteins Gal-BSA and GlcNAc-BSA were added to a final concentration of 0.2 mg/ml. Monosaccharides and EDTA were added to a final concentration of 2 and 10 mM, respectively.

Preparation of MDBK cell PMVs, MDBK cell homogenates, and PMV extracts

PMV were generated from MDBK cells using modifications of a previously described procedure (Scott, 1976). Briefly, MDBK cells were grown to confluency in 150-cm^2 flasks at 37 C in a 5% CO_2 incubator. Cell monolayers (approximately 2×10^8 cells total) were exposed to PBS containing 250 mM formaldehyde and 2 mM dithiothreitol for 3 hr at 37 C in a 5% CO_2 incubator. After this incubation, PMVs were decanted from the confluent monolayer, washed by centrifugation at 30,000 *g* for 30 min, resuspended in 1-ml MEM (without serum), and stored at 4 C until use in binding assays.

MDBK cell homogenates were prepared as follows. Monolayers of MDBK cells were grown past confluency in MEM with 10% horse serum at 37 C in a 5% CO_2 incubator. Media were decanted from the flasks (185-cm^2, Nunclon plates, Fisher Scientific), and monolayers were rinsed with PBS. Monolayers were scraped from the flasks (5 at a time) using a plastic cell scraper into approximately 7 ml of aqueous extraction buffer (pH 7.3) containing 100 mM HEPES, 1 M NaCl, 0.2 mM EDTA, 0.2 mM dithiothreitol, 6 mg/L deoxyribonuclease, 0.5%

sodium cholate, and 2% Protease Inhibitor Cocktail (for Mammalian Cell Extracts). Cells scraped from 15 flasks (approximately 7.5×10^8 cells) were pooled, homogenized, and centrifuged at 600 *g* for 5 min. Pellets containing cell nuclei and debris were discarded, and supernatants were stored at −20 C. Before use in lipid purification, the pooled supernatants from 100 flasks of homogenized cells were thawed and centrifuged at 100,000 *g* for 60 min at 4 C in a Ti70 rotor (Beckman Instruments, Fullerton, California). This supernatant, along with aliquots of original cell homogenate, was exhaustively dialyzed against water, lyophilized, and resuspended in a minimal volume of water before HPLC or HPTLC purification. Alternatively, aqueous extracts of MDBK cells were also prepared by scraping monolayers directly into water (approximately 15 ml per fifteen 185-cm^2 flasks), homogenizing, and storing at −20 C. The sporozoite-binding inhibitory activity of these various extracts was determined by mixing with an appropriate volume of 10 × PBS and tested in the standard binding assay.

For initial extraction of plasma membranes, PMVs were suspended in MEM at 4 C and disrupted by pulse sonication using a probe sonicator (Heat Systems-Ultrasonics Inc., Fermingdale, New York) at 50% power or by homogenization in a Dounce tissue grinder until intact vesicle was no longer apparent by microscopic observation.

MDBK cell homogenate or PMV treatments

Aliquots of PMV or MDBK cell homogenates were treated with heat, proteases, neuraminidase, and glycosidases, as described below, to probe the chemical nature of the sporozoite-binding inhibitory activity contained in these fractions. Duplicate control tubes, containing only MDBK cells or PMV and sporozoites, were processed simultaneously, and sporozoite-binding inhibitory activity was determined for each of the treated MDBK cell or PMV extracts by comparison with these separate control incubations.

Aliquots of MDBK cell or PMV extracts were placed into 1.5-ml microfuge tubes in a boiling water bath for 15 min. After allowing the tubes to cool to approximately 4 C, sporozoites and MDBK cells were added to the tubes, and the standard binding assay was performed as described previously.

The proteases trypsin (TPCK treated, Type XIII from bovine pancreas), Pronase (crude protease, Type I from bovine pancreas), and proteinase K (Type XI from *Tritirachium album*) were each prepared at a concentration of 10 mg/ml in PBS. Aliquots of each protease, and a PBS control, were pretreated for 1 hr at 37 C in a shaking water bath to destroy any glycosidase activity. Aliquots (300 μl) of MDBK cell or PMV extracts in water containing 10% 10 × PBS were mixed with 35 μl of each protease, as well as PBS (control), and incubated in a shaking water bath for 14 hr at 37 C. After incubation, the tubes were cooled and the contents transferred to 1.5-ml microfuge tubes. The protease-treated extracts were then boiled for 5 min (conditions that did not inactivate sporozoite-binding inhibitory activity) to deactivate any remaining enzyme. Extracts were then held on ice before being tested in the standard binding assay.

The following incubations were carried out in borosilicate culture tubes (12 × 75 mm) at 37 C using a shaking water bath. Aliquots of MDBK cell or PMV extracts were incubated at 37 C for 60 min with 105-mU neuraminidase (from *Clostridium perfringens*) in 200-mM sodium acetate buffer (final concentration 20 mM sodium acetate, pH 6.0) and then boiled for 5 min. An aliquot of this incubation mixture was then stored at 4 C overnight. Another aliquot was incubated overnight with 6-mU *O*-glycosidase (from *Diplococcus pneumoniae*, Boehringer Ingelheim, Danbury, Connecticut), whereas another aliquot was incubated with 9-U *N*-glycosidase F (recombinant, Boehringer Ingelheim). An aliquot of MDBK cell or PMV extract (not treated with neuraminidase) was incubated with 9-U *N*-glycosidase F in 20 mM Na_2HPO_4 buffer (pH 7.2). An aliquot of MDBK cell or PMV was also simultaneously

incubated with 9 U of *N*-glycosidase F, 6 mU of *O*-glycosidase, and 9 mU of neuraminidase in Na_2HPO_4 buffer (pH 7.2). After all incubations, tubes were boiled for 5 min and stored on ice. Sham-treated (no enzymes) controls were processed simultaneously. Fetuin (1 mg/ ml), incubated exactly as described above for MDBK cell or PMV extracts, was used as the positive control for *N*- and *O*-glycosidase digestions. For these control incubations, fetuin molecular mass was monitored before and after glycosidase digestion by sodium dodecyl sulfate–polyacrylamide gel electrophoresis. After the various treatments, sporozoites and MDBK cells were added to all incubation volumes, and the binding assay was performed as described previously.

Organic solvent extraction of MDBK cells and PMV

Monolayers of MDBK cells (approximately 5.25×10^9 cells) were grown past confluency in MEM as described above. Media were decanted from the flasks, and monolayers were rinsed with PBS. Monolayers were scraped from the flasks using a plastic cell scraper into a minimal volume of water, homogenized with a Dounce tissue grinder, and stored at −20 C. Cell homogenates in water were thawed, and 36 ml was placed in each of the four 250-ml polypropylene bottles (Nalgene, Fisher Scientific). Organic solvent extraction was performed as follows: 96 ml of methanol and 48 ml of chloroform (chloroform:methanol:water, 4:8:3) were added to each bottle containing the cell homogenate and mixed well by vortexing. After centrifugation at 1,000 *g* for 10 min (Sorvall Superspeed RC2-B, GSA rotor; Kendro Laboratory Products, Newtown, Connecticut), supernatants were pooled and partially evaporated with a rotary evaporator. The remaining aqueous phase (38.3 ml) was dialyzed (12–14,000 molecular weight cut off) against 100,000 volumes of water. After exhaustive dialysis, the extract was lyophilized and resuspended in a total volume of 10 ml chloroform and methanol (2:1).

In addition, MDBK cells and PMVs derived from MDBK cells as described above were extracted with chloroform:methanol (30:1). Aliquots of aqueous extracts of MDBK cells prepared by scraping monolayers directly into water (as described above) and aliquots of freshly prepared PMVs were placed in 30-ml glass centrifuge tubes and mixed with 6 ml of chloroform:methanol (30:1). Pulse sonication with a probe sonicator was performed at 50% power for three 1-min intervals. Tubes were then centrifuged at 1,500 *g* for 10 min. The bottom chloroform layer was collected, whereas the upper water layer resting on a narrow band of denatured protein was discarded. Chloroform layers were pooled and dried in a Speed Vac (Savant SC 110A, Fisher Scientific).

Collection and organic solvent extraction of bovine mucosa

A 5-day-old male Holstein calf was obtained from the University of Illinois Dairy and killed by intravenous injection of barbiturate. The small intestine was excised and rinsed thoroughly with chilled PBS. The intestine was opened, and the mucosa was removed by gently scraping with a glass microscope slide. The mucosal scrapings were washed thrice with PBS and stored at −80 C pending extraction. Aliquots of bovine mucosa that had been stored at −80 C were thawed and homogenized with a tissue grinder. Aliquots (2 ml) of homogenized mucosa were placed in 30-ml glass centrifuge tubes and mixed with 6 ml of chloroform:methanol (30:1). Pulse sonication with a probe sonicator was performed at 50% power for three 1-min intervals. Tubes were then centrifuged at 1,500 *g* for 10 min. The bottom chloroform layer was collected, whereas the upper water layer resting on a narrow band of denatured protein was discarded. The narrow band of denatured protein was then mixed with 6 ml of chloroform:methanol (30:1) and pulse sonicated again for three 1-min intervals. Centrifugation followed by collection of the chloroform layer was repeated as described previously. Chloroform layers were pooled and dried by evaporation.

Purification of a sporozoite-binding inhibitory lipid from bovine mucosa

Organic solvent extracts of bovine mucosa (extracted in chloroform: methanol, 30:1) were dissolved in chloroform:methanol (2:1). Aliquots (500 μl) were individually filtered through 0.45-μm nylon centrifuge filters (Alltech, Deerfield, Illinois) by microcentrifugation, and the filters were rinsed with 500-μl aliquots of solvent. Filtrates were evaporated and dissolved in 1-ml equilibrating solvent (chloroform:methanol, 40: 1). These extracts were chromatographed on a Dionex DX-300 HPLC system (Dionex Corp., Westmont, Illinois) equipped with an Econosil semipreparative silica column (Alltech, 10 nm particles, 10 × 250 mm). After equilibration in solvent 1, (chloroform:methanol [40:1]), at a flow rate of 2 ml/min, the extract (equivalent to approximately 8 ml of original bovine mucosa homogenate) was redissolved in 1-ml equilibrating solvent and injected into a 1-ml sample loop. A computer program was used to control the solvent gradients. The eluant composition was held stable at 100% solvent 1 for 60 min followed by a 60-min linear gradient from 100% solvent 1 to 100% solvent 2 (chloroform:methanol: water [60:35:8]). The final 60 min were run at 100% solvent 2. Continuous monitoring and collection of eluted lipid peaks was performed by evaporative light-scattering detection (Alltech) coupled with 98% split-stream fraction collecting using a Gilson FC203 fraction collector. Collected fractions were evaporated to dryness, dissolved in chloroform:methanol, 2:1, and aliquots analyzed by TLC and HPTLC to confirm the presence and assess purity of the inhibitory lipid.

TLC, HPTLC, and semipreparative HPTLC

The HPLC fractions with the active lipid band were streaked onto HPTLC plates for final purification. Dried samples were dissolved in chloroform:methanol (2:1) and streaked on either TLC (Merck) or HPTLC (Merck) plates. Appropriate volumes, generally 5 μl/lane, of sample were spotted in 0.5-cm streaks (separated by 1.0-cm blank lanes on HPTLC plates). Plates were developed in 30:1 chloroform:methanol, sprayed with primulin reagent (0.01% primulin in acetone:water, 4:1), and observed under UV light to detect lipid bands. For semipreparative HPTLC, samples were streaked onto the entire widths of multiple silica gel TLC plates (Merck) or multiple HPTLC plates (Merck) using a manual TLC Streaker (Alltech). After development, the outer vertical edges of the plates were stained with primulin, and the unstained middle portion of the lipid bands were scraped from the plates, eluted in chloroform:methanol:water 30:60:20, and dried by evaporation. Comparable blank lanes were also scraped from the plates and identically processed to serve as negative controls in the sporozoite-binding assay.

Physical–chemical characterization of the purified inhibitory lipid

TLC staining—The purified inhibitory lipid and controls (organic solvent extracts of MDBK cells or mucosa, cholesterol, cholesterol-3-sulfate, PE, PC, glucocerebroside, and GM_3 ganglioside) were streaked on TLC plates and developed as described above. Plates were sprayed with 0.01% primulin in acetone:water (4:1), fluorescamine (0.15% in dry acetone), orcinol (0.2% in 2 M H_2SO_4), orcinol ferric chloride (0.9% ferric chloride and 55% orcinol in acidified ethanol solution), resorcinol (0.2% in concentrated HCl), molybdenum blue (1.3% molybdenum oxide in 4.2 M H_2SO_4), Phospray, or antimony trichloride (22%, in chloroform). Primulin- and fluorescamine-sprayed plates were examined under UV light, and others were heated to 100 C for 10 min to observe bands.

Dialysis—Approximately 20 μg of the purified lipid was resuspended in 200 μl using a water bath sonicator. The sample was transferred to a Slide-A-Lyzer Mini Dialysis Unit (Pierce, Rockford, Illinois) and exhaustively dialyzed against water. A sham-treated control was processed in the same manner but was only transferred into the dialysis unit and not actually dialyzed. Samples were removed from the dialysis units and the units rinsed twice with water. The samples, including water rinses, were placed into 6 × 50–mm borosilicate tubes and

evaporated to dryness. Samples, including 20 μg of undialyzed lipid as a control, were dissolved in 17-μl chloroform:methanol (2:1) and various amounts spotted on TLC plates. After development in chloroform:methanol (30: 1), plates were sprayed with 0.01% primulin, and bands were observed under UV light. The amount of lipid recovered before and after dialysis was quantified by densitometry using an Alpha Innotech digital imaging system (Alpha Innotech, San Leandro, California).

Heat—Twenty micrograms of the purified lipid was dissolved in 200-μl water in a 1.5-ml plastic microfuge tube and boiled for 15 min. Sham-treated (no boiling) controls were processed simultaneously. The contents of the microfuge tubes were then transferred to 6 × 50–mm borosilicate tubes and evaporated to dryness in a Speed Vac. The samples were dissolved in a small volume of chloroform:methanol (2:1) and spotted on TLC plates. After development in chloroform:methanol: water (60:30:4.5) and chloroform:methanol (30:1), plates were sprayed with 0.01% primulin and examined under UV light.

Ceramide glycanase digestion—Twenty micrograms of the purified inhibitory lipid was dissolved in 100 μl of ceramide glycanase buffer (100 μl of sodium acetate, 1 M, pH 5.0), 250 μl of sodium taurodeoxycholate in water (2 mg/ml), 100 μl of sodium cholate in water (20 mg/ml), 550 μl water, and 0.5 U ceramide glycanase (V-Labs Inc., Covington, Louisiana). Sham-treated (no ceramide glycanase) samples and aliquots of GM_3 ganglioside (positive control) were processed simultaneously. All incubation tubes were placed in a 37 C water bath for 70 hr. After incubation, the samples were processes as described for heat treatment.

Periodate oxidation—Twenty micrograms of the purified lipid was dissolved in 50 μl of periodate reagent (10 mM sodium metaperiodate in 10 mM sodium acetate, pH 4.5). A control sample was dissolved in 10-mM sodium acetate buffer alone. GA_2 ganglioside was used as the positive control. All tubes were incubated at 4 C for 16 hr in the dark. After incubation, each tube was extracted with methanol (67 μl) and chloroform (133 μl). Tubes were centrifuged at 1,000 *g* for 10 min to separate the layers. The water layers were decanted, placed in separate tubes, and evaporated to dryness. The dried water layers were again extracted with methanol (67 μl), chloroform (133 μl), and water (50 μl) and centrifuged to separate the layers. The bottom layers from both extractions were pooled, evaporated to dryness, redissolved in chloroform:methanol (2:1), and chromatographed on TLC plates as described above.

Mild base hydrolysis—Twenty micrograms of the purified lipid, as well as aliquots of phosphatidylethanolamine, phosphatidylserine, and phosphatidylinositol, was dissolved in 100 μl of 14.8-M NH_4OH. Tubes were incubated at 37 C for 90 min. Control samples were incubated without the addition of NH_4OH. After incubation, tubes were evaporated to dryness, redissolved in chloroform:methanol (2:1), and chromatographed on TLC plates as described above.

Mass spectrometry—Fast atom bombardment mass spectrometry of the purified lipid was performed in the Mass Spectrometry Laboratory, School of Chemical Sciences, University of Illinois, Champaign, Illinois. Low-resolution fast atom bombardment was performed with a ZAB-SE spectrometer. A 3:1 mixture of dithiothreitol and dithioerythritol was used as the matrix. Approximately 1.2 mg of purified lipid was evaporated to dryness and submitted for analysis at a resolution of 1,000 and a scan mass range of 0–1,000. High-resolution fast atom bombardment mass spectrometry was performed with a 70-SE-4F mass spectrometer. Analysis was performed at a resolution of 10,000.

Elemental analysis—Elemental analysis of the purified lipid was performed at the Microanalysis Laboratory, School of Chemical Sciences, University of Illinois, Champaign,

Illinois. Carbon, hydrogen, and nitrogen were measured with a Carbon, Hydrogen, Nitrogen Analyzer (CHN, CE440 by Exeter Analytical Inc., N. Chelmsford, Massachusetts). Metallic elements were measured with Inductively Coupled Plasma (ICP, PlasmaII by Perkin–Elmer, Norwalk, Connecticut). Approximately 2 mg of MIC was evaporated to dryness and submitted for CHN and ICP analysis. For ICP analysis, the sample was digested with an MDS-2000 (Microwave Digestion System, CEM, Charlotte, North Carolina) with nitric acid and hydrochloric acid at high temperature and pressure (125 psi).

Additional lipids tested in sporozoite-binding assays—The following lipids were sonicated in 100-μl MEM and tested for inhibitory activity within the standard binding assay: cholesterol, dihydrocholesterol, cholesterol 3-SO_4, cholesteryl-*n*-butyrate, cholesteryloleate, cholesterylpalmitate, cholesterylmyristate, cholesterylaniline, ceramide, glucocerebroside, galactocerebroside, and PE. Cholesterol and cholesterol derivatives were added at a final concentration ranging from 0.1 to 0.7 mg/ml. Ceramide was added at a concentration of 0.3 mg/ml. The cerebrosides were added at a final concentration of 0.1 mg/ml, and PE was added at a final concentration of 0.15 mg/ml.

RESULTS

Validation of in vivo relevance of the sporozoite-binding assay

Rapid sporozoite–host cell binding was observed at 37 C and was maximized at 20 min, with the extent of binding ranging from 40 to over 250 sporozoites bound per 100 MDBK cells (Fig. 1). Most cells with bound sporozoites contained 1 or 2 attached sporozoites; however, we have occasionally seen as many as 5 sporozoites bound to a single MDBK cell. The extent of binding varied between sporozoite preparations. For most sporozoite preparations, binding rates were reproducible at 40–60 binding events per 100 cells at 20 min of incubation. At 4 C, sporozoites did not bind to host cells. The maximal adhesion observed at 20 min at 37 C was followed by a marked reduction in sporozoite binding. Although there is increased difficulty in observing sporozoites attached to MDBK cells with increasing incubation time, because of invasion and embedding of the sporozoite deeper into the host cell membrane, this phenomenon does not explain the rapid loss of sporozoite binding seen after 20 min. Preincubation of sporozoites alone in MEM at 37 C for 60 min caused a time-dependent loss of more than 80% of their host cell–binding activity when subsequently mixed with MDBK cells in the standard binding assay (data not shown).

These adhesion kinetics were qualitatively identical regardless of a variety of host cell types (Caco-2, HT-29, MA-104, human foreskin fibroblasts, murine neuroblastoma, adult canine erythrocytes, and neonatal bovine erythrocytes) examined in our binding assay. The greatest binding was seen with MDBK cells and sporozoites used immediately after excystation. Although, *C. parvum* appears to prefer intestinal cells or cell lines for intracellular development (Upton et al., 1994), our observed lack of host cell adhesive specificity is similar to previously published results demonstrating that a variety of intestinal and nonintestinal cells, including monocytes, can be infected (Lawton et al., 1997; Yu et al., 2000). Accordingly, MDBK cells were routinely used throughout the rest of this study because of their high sporozoite-binding activity, relative ease of culture manipulations, and maintenance of high viability during cell suspension incubations. Although the number of sporozoites bound per 100 MDBK cells varied depending on the particular sporozoite preparation, the percentage inhibition of binding, displayed by a particular inhibitory fraction or negative control (see below), was remarkably reproducible between replicates within each experiment (<10% variation from experiment to experiment).

The morphological characteristics of the adhesion of sporozoites to MDBK cells were documented by phase contrast and electron microscopy (Figs. 2, 3, respectively). The typical

curved shape of the sporozoite was still recognizable at early time points, but at longer times (20–30 min), sporozoites appeared to embed deeper into host cells and lose their elongated shape. They formed a more rounded or somewhat blunted shape on the surface of the MDBK cell. Hallmark ultrastructural features characteristically seen during in vivo sporozoite adhesion and invasion of intestinal epithelial cells (Bird and Smith, 1980;Current and Reese, 1986;Fayer et al., 1997) were also evident during in vitro adhesion to MDBK cells in suspension. Electron microscopic examination (Fig. 3) demonstrated the formation of a parasitophorous vacuole, the presence of a typical electron-dense layer at the adhesive junction between the sporozoite and MDBK cell, anterior invagination of the sporozoite plasma membrane, and concomitant development of an electron-dense collar. These same morphological features observed during sporozoite adhesion to MDBK cells in suspension were also seen for all the other cell types examined, including primary bovine enterocytes (data not shown).

Screening for inhibitors of sporozoite binding

Previous studies (Thea et al., 1992; Barnes et al., 1998; Gut and Nelson, 1999; Kelly et al., 2000; Cevallos et al., 2000) have implicated sporozoite glycoconjugates, especially mucins or mucinlike proteins and lectinlike activity, as being involved in sporozoite attachment or invasion. As an initial screen to help identify the type of host cell surface chemistry that may be exploited during sporozoite recognition and adhesion, we examined a variety of glycoconjugates, representative of some of the carbohydrate epitopes frequently found on mammalian host cell surfaces, for their ability to inhibit sporozoite binding to MDBK cells. Only mucins, including commercial preparations of porcine gastric and bovine submaxillary mucins, as well as calf abomasal mucin, notably inhibited sporozoite binding (Fig. 4). Of the other glycoconjugates tested, 2 neoglycoproteins, GlcNAc-BSA and Gal-BSA, also had an inhibitory effect, although to a lesser extent than the mucins. A GalNAc-terminated globoside (4-globoside), fetuin, orosomucoid, and millimolar concentrations of GlcNAc did not inhibit sporozoite binding. Slight inhibition was observed by high concentrations (2 mM) of GalNAc and may be related to mucin inhibition because GalNAc is a prominent monosaccharide component of mucins. The galactose-terminated disaccharide, Gal(α1–4)Gal, represented in 3-globoside or ceramide trihexoside, showed no ability to inhibit sporozoite attachment to MDBK cells. Polysialic acid (colominic acid), porcine GM_3 ganglioside, sialyllactose, and glycosaminoglycans also showed no inhibitory effect. Binding also was not significantly inhibited by excess BSA or by the presence of EDTA.

PMVs inhibit sporozoite binding to host cells

The results of our glycoconjugate screen suggested that mucins may be a candidate receptor for *C. parvum* sporozoite adhesion. Furthermore, specific carbohydrate epitopes found in mucins have been previously implicated as potential receptors for *C. parvum* adhesion to epithelial cells (Thea et al., 1992; Joe et al., 1994; Barnes et al., 1998; Joe et al., 1998; Cevallos et al., 2000). Because mucins are clearly present along the luminal surface of the intestinal tract, it is reasonable to assume that they could be involved in sporozoite recognition of host cells. Epithelial cell surface molecules other than mucins, however, also may be involved in these interactions because, in particular MDBK cells, as well as MA-104 tissue culture cells, adult canine erythrocytes, and neonatal bovine erythrocytes, are not known to synthesize mucins yet are readily bound by sporozoites. To investigate whether a mucin, mucinlike, or other host cell surface molecule functions as a host cell surface receptor for *C. parvum* sporozoites, we began to isolate and fractionate MDBK cell plasma membranes. In an attempt to initially preserve MDBK cell plasma membrane topology, our initial cell fractionation involved preparation of right-side-out PMVs, as described previously (Scott, 1976). Characterization of these vesicles by phase contrast and electron microscopy (Fig. 5) revealed that they are variably sized membrane vesicles, devoid of subcellular organelles, and have the

morphological characteristics previously described for plasma membranes (Scott, 1976). We tested these PMVs for sporozoite-binding inhibitory activity. Both native and sonication-disrupted vesicle preparations exhibited marked inhibitory activity when tested in the standard binding assay (Fig. 6). Furthermore, electron microscopic examination of aliquots of sporozoites incubated with PMV in the absence of MDBK cells indicated that sporozoites bind to PMVs (Fig. 5). Interestingly, whereas some morphologic features of the initial sporozoite attachment to intact MDBK cells, such as a beginning anterior invagination of the sporozoite plasma membrane, were observed in the sporozoite–PMV interaction, other characteristics of sporozoite–host cell invasion were not apparent when sporozoites adhered to PMV. For example, the formation of an early parasitophorous vacuole, the electron-dense layer, and the electron-dense collar were not seen. These findings suggested that PMV could inhibit sporozoite binding by competing with MDBK cells for sporozoite-binding sites. Furthermore, the resistance of sporozoite-binding inhibitory activity of PMV to sonic disruption suggested that the activity was stable and thus amenable to further purification and characterization.

During initial purification of the inhibitory activity from aqueous homogenates of both PMV and MDBK cells, the activity displayed a polydisperse profile during conventional ion exchange and gel filtration chromatography. Furthermore, the inhibitory activity was not affected by heat or a variety of proteases, neuraminidase, and other glycosidases (data not shown). These results indicated that the activity might be lipid in nature. Therefore, organic solvent extraction of MDBK cell homogenates was performed. These extracts exhibited pronounced sporozoite-binding inhibitory activity and represented approximately 60% of the total activity seen in an equivalent amount of crude MDBK cell aqueous homogenate (Fig. 7).

Purification of sporozoite-binding inhibitory activity

Initial purification of organic solvent extracts of MDBK cells by preparative TLC yielded 2 major inhibitory fractions, a polar lipid fraction and a nonpolar lipid fraction. The nonpolar fraction, which migrated near the solvent front in a relatively polar solvent system (60:30:4.5), contained the major inhibitory activity (data not shown). This nonpolar fraction contained 3 components that were separable by TLC using a chloroform:methanol (30:1) solvent system. This solvent system was then used to purify larger amounts of the inhibitory lipid from organic solvent extracts of bovine mucosa using a combination of HPLC and preparative TLC. Briefly, active HPLC fractions were subjected to semipreparative TLC, individual bands scraped from the plates, eluted from the silica, tested for inhibitory activity in the standard binding assay (TLC-extracted blank lanes and noninhibitory bands, such as cholesterol and phosphatidylethanolamine, served as negative controls), and rechromatographed on HPTLC plates to verify purity. A major, lipid-staining band was recovered from final TLC plates and contained approximately 80% of the sporozoite-binding inhibitory activity initially applied (Fig. 8). The material also chromatographed as a single TLC band in 2 other solvent systems, further demonstrating the purity of the final preparation (data not shown).

To demonstrate that the purified lipid was acting on sporozoites rather than host cells, we performed preincubation studies. We saw no effect when host cells are preincubated with the highest concentrations of inhibitors (lipid fractions) for 60 min at 37 C, washed free of the inhibitor, and then incubated with freshly excysted sporozoites (data not shown).

Initial characterization of inhibitory lipid

The results of TLC staining techniques (Table I) using orcinol spray reagents did not reveal the presence of carbohydrate. The lipid was also not stained with resorcinol or fluorescamine, suggesting the absence of sialic acid or primary amine groups. No phosphorus was found with Phospray or molybdenum blue stain. The lipid also failed to stain with antimony trichloride, a reagent used for the identification of steroid glycosides, vitamin A, or related steroid ring

structures. Furthermore, cholesterol and several cholesterol derivatives, ceramide, glucocerebroside, galactocerebroside, and phosphatidylethanolamine, demonstrated no significant inhibitory activity in the binding assay (data not shown).

The binding inhibitory activity and TLC behavior of the purified lipid was also unaffected by heat, ceramide glycanase digestion, periodate oxidation, or mild base hydrolysis. Elemental analyses for carbon, hydrogen, nitrogen, and metallic elements detected only carbon (78%) and hydrogen (12%). Low-resolution fast atom bombardment mass spectrometry showed a relatively large (M+H)+ peak measuring 459.3 amu. A smaller (M+Na)+ sodium salt peak at 481 amu was also identified. A summary of the results of the various physical and chemical analyses performed is shown in Table I.

DISCUSSION

Our investigation of *C. parvum* sporozoite–host cell early adhesion events required the design of a physiologically relevant assay to rapidly measure specific binding events. The assay incubation conditions we have described here gently tumble the cells together, mimicking the shear forces of fluids during gut peristalsis and minimizing nonspecific attachment. By adding exogenous substances to this incubation, we are able to examine the effects of potential inhibitors of adhesion (putative receptors). We have shown that the morphological changes seen in sporozoites attaching to MDBK cells during in vitro–binding assay conditions are characteristic of those seen in invading sporozoites during tissue infection in vivo (Bird and Smith, 1980; Current and Reese, 1986; Fayer and Ungar, 1986; Lumb et al., 1988; Fayer, 1990; Yoshikawa and Iseki, 1992; Thulin et al., 1994; Fayer et al., 1997). These results demonstrate the biological relevance of our in vitro–binding assay to the microbial adhesion process occurring in natural infections.

The results of our initial glycoconjugate screen suggested that mucins may be a candidate receptor for *C. parvum* sporozoite adhesion and supported previous studies implicating mucins as possible receptors for sporozoite adhesion to epithelial cells (Thea et al., 1992; Joe et al., 1994; Barnes et al., 1998; Joe et al., 1998; Cevallos et al., 2000). We were interested, however, in exploring the possibility that other cell surface molecules are also likely involved in the early adhesion process because MBDK cells do not synthesize or secrete mucins during in vitro growth. Consequently, our goal in this study was to identify, by classical biochemical methods, possible host cell surface receptors for *C. parvum* and to evaluate whether molecules other than mucins were involved in sporozoite adhesion or invasion. We began by examining whether PMVs and aqueous extracts of MDBK cells could inhibit sporozoite adhesion. Both membrane vesicles and MDBK cell extracts inhibited sporozoite adhesion in a dose-dependent manner when added exogenously during binding assays. These results suggested that a host cell surface molecule may be required for at least the initial sporozoite–host cell recognition event. One such candidate receptor molecule has recently been detected and partially characterized from bovine intestinal mucosa (Langer et al., 2001). In addition, somewhat serendipitously, we discovered that sporozoites can bind PMV but cannot proceed with the subsequent stages of invasion. Thus, PMV can be used to experimentally separate the processes of sporozoite adhesion from invasion and should be a valuable tool in deciphering the molecular mechanisms of initial sporozoite recognition and adhesion.

To further characterize the sporozoite-binding inhibitory activity we detected in aqueous extracts of membrane vesicles and MDBK cells, we fractionated these extracts to begin purifying a putative sporozoite receptor on the basis of its sporozoite-binding inhibitory activity. Initial attempts to purify an inhibitory fraction by ion exchange or gel filtration chromatography were not successful because the inhibitory activity dispersed among multiple column fractions. This behavior suggested either the presence of multiple inhibitors or that the

inhibitor activity was not completely soluble in aqueous buffers, unusual for a protein but typical of lipids. Furthermore, the failure of proteases, neuraminidase, glycosidases, or heat to destroy the inhibitory activity suggested that a lipid component may be responsible for the sporozoite-binding inhibitory activity. Subsequent organic solvent extracts of both MDBK cells and PMVs retained the majority of the inhibitory activity as compared with aqueous extracts and thus we further fractionated the organic extracts by TLC and examined each separate band for activity. A single band was found to possess more than 80% of the inhibitory activity of the entire organic extract. Using the same organic solvent extraction and purification procedure developed for PMV and MDBK extracts, we were able to purify the same lipid component in relative large amounts from bovine intestinal mucosa. We have initially characterized this inhibitory lipid as a nonsteroidal, nonsaponifiable lipid lacking carbohydrate and phosphate moieties. The molecular mass of 459 Da, and a composition of carbon and hydrogen with no nitrogen, phosphorous, or carbohydrate, suggests that this lipid is a form of long-chain hydrocarbon including lipid classes such as cholic acids, long-chain fatty acids, or fatty alcohols, eicosanoids, or steroids, such as the cholesterols. Cholesterol derivatives migrate similarly to our lipid in some solvent systems; however, on direct assay of numerous of these derivatives, none of them inhibit sporozoite binding. Furthermore, the purified lipid does not stain for the presence of a steroid ring structure. We are currently analyzing the purified lipid by carbon and proton 2-dimensional nuclear magnetic resonance and high-resolution mass spectrometry. Despite the lack of complete structural data, our results suggest that a lipid present in the bovine intestine may play a critical role in *C. parvum* infectivity of the intestinal epithelium.

As mentioned previously, the results of our initial glycoconjugates screen, as well as numerous reports from other investigators (Petersen et al., 1997; Barnes et al., 1998; Cevallos et al., 2000), suggest the involvement of mucins in *C. parvum* sporozoite adhesion to host cells. The isolation of a sporozoite-binding inhibitory lipid molecule from MDBK cells and from bovine intestinal mucosa suggests that a lipid, or lipid-like, molecule may also be involved in sporozoite–host cell interactions. A possible mechanism to explain the involvement of both types of molecule in the overall microbial adhesion process is that mucins may act as an early, relatively low affinity sequestration receptor for sporozoites, whereas the lipid we have isolated is involved in the later process of attachment to the enterocyte surface. Sporozoite surface lectins may initially recognize mucins by way of interaction with specific carbohydrate epitopes, such as *N*-acetyl galactosamine residues (Gut and Nelson, 1999), or mucins may simply trap sporozoites because of their viscous, gel-like nature. This initial interaction along the gut mucosal surface, which is likely part of a dynamic, multiple receptor pathway, may serve to retard sporozoite transit and bring them in close proximity with additional enterocyte receptors, such as the putative lipid-like molecule we have isolated in this study. Alternatively, although this molecule may be a lipid or part of a lipid domain of a receptor involved in host cell recognition, it is also possible that it is acting by a receptor-independent mechanism such as a signaling molecule not directly involved in host cell attachment.

Several studies have demonstrated inhibitory effects of specific lipids on protozoan parasites. Yong and others reported that the generation of thromboxane by host platelets damaged *Toxoplasma gondii* membranes, possibly as a defense against the parasite (Yong et al., 1991). Two of these authors later showed that 13-HODE released by platelets was cytotoxic to *T. gondii* (Henderson et al., 1992). The release of leukotriene B4 by mast cells after exposure to *T. gondii* also resulted in damage to the parasites (Henderson and Chi, 1998). Although the inhibitory lipid we have isolated does not appear to be cytotoxic to *C. parvum*, it may influence adhesion in a different fashion, perhaps by stimulation of intracellular signaling pathways. In *Trypanosoma brucei*, the addition of exogenous arachidonic acid stimulated the release of Ca^{2+} from intracellular stores at a range of 10–75 μM (Catisti et al., 2000). We plan to

investigate possible effects of the inhibitory lipid on calcium flux in *C. parvum* in future experiments.

Although we have by no means ruled out the involvement of host cell surface protein receptors, we have shown that a lipid, found naturally in the calf intestinal mucosa, inhibits the adhesion of *C. parvum* sporozoites to MDBK cells. Purification of relatively large amounts of the active lipid from bovine mucosa, followed by further chemical and structural characterization studies, as well as determination of its mechanism of inhibition of sporozoite adhesion, may ultimately provide an avenue for its use as a natural therapeutic competitor to block infectivity of this unique pathogen in vivo.

Acknowledgements

The AUCP-1 isolate of *C. parvum* used in these studies was originally a gift from Byron Blagburn, Auburn University. The HT-29 (human colonic carcinoma) cell line was a gift from Rex Gaskins, University of Illinois. Human newborn foreskin fibroblasts and murine neuroblastoma cells were a gift from Milton McAllister, University of Illinois. Neoglycoproteins were generously donated by Y. C. Lee, Johns Hopkins University. S-colominic acid was a gift from Shinya Yamaguchi, Kyoto Research Laboratories, Marukin Shoyu Co., Ltd., Kyoto, Japan. Sialyllactose was a gift from Steven Roth, Neose Technologies Inc., Horsham, Pennsylvania. Porcine GM_3 ganglioside was a gift from Theresa Kuhlenschmidt, University of Illinois (Rolsma et al., 1998). This work is supported by National Institutes of Health Grant AI 44967-01A1, and USDA regional research funds (NC 1007).

LITERATURE CITED

Barnes DA, Bonnin A, Huang JX, Gousset L, Wu J, Gut J, Doyle P, Dubremetz JF, Ward H. A novel multi-domain mucin-like glycoprotein of Cryptosporidium parvum mediates invasion. Molecular and Biochemical Parasitology 1998;96:93–110. [PubMed: 9851610]

Bird RG, Smith MD. Cryptosporidiosis in man: Parasite life cycle and fine structural pathology. Journal of Pathology 1980;132:217. [PubMed: 7431158]

Catisti R, Uyemura SA, Docampo R, Vercesi AE. Calcium mobilization by arachidonic acid in trypanosomatids. Molecular and Biochemical Parasitology 2000;105:261–271. [PubMed: 10693748]

Cevallos A, Bhat N, Verdon R, Hamer DH, Stein B, Tzipori S, Pereira ME, Keusch GT, Ward HD. Mediation of *Cryptosporidium parvum* infection in vitro by mucin-like glycoproteins defined by a neutralizing monoclonal antibody. Infection and Immunity 2000;68:5167–5175. [PubMed: 10948140]

Chen XM, LaRusso NF. Mechanisms of attachment and internalization of *Cryptosporidium parvum* to biliary and intestinal epithelial cells. Gastroenterology 2000;118:236–379.

Current, WL. Techniques and laboratory maintenance of *Cryptosporidium*. In: Dubey, JP.; Speer, CA.; Fayer, R., editors. Cryptosporidiosis of man and animals. CRC Press; Boca Raton, Florida: 1990. p. 31-49.

Current WL, Reese NC. A comparison of endogenous development of three isolates of *Cryptosporidium* in suckling mice. Journal of Protozoology 1986;33:98. [PubMed: 3959014]

Current WL, Reese NC, Ernst JV, Bailey WS, Heyman MB, Weinstein WM. Human cryptosporidiosis in immunocompetent and immunodeficient persons. Studies of an outbreak and experimental transmission. New England Journal of Medicine 1983;308:1252–1257. [PubMed: 6843609]

Fayer, R. General biology of *Cryptosporidium*. In: Dubey, JP.; Speer, CA.; Fayer, R., editors. Cryptosporidiosis of man and animals. CRC Press; Boca Raton, Florida: 1990. p. 1-29.

Fayer, R.; Speer, CA.; Dubey, JP. The general biology of *Cryptosporidium*. In: Fayer, R., editor. Cryptosporidium and cryptosporidiosis. CRC Press; Boca Raton, Florida: 1997. p. 1-41.

Fayer R, Ungar BLP. *Cryptosporidium* spp and cryptosporidiosis. Microbiological Reviews 1986;50:458–482. [PubMed: 3540573]

Gut J, Nelson RG. *Cryptosporidium parvum*: Synchronized excystation in vitro and evaluation of sporozoite infectivity with a new lectin-based assay. Journal of Eukaryotic Microbiology 1999;46:56S–57S. [PubMed: 10519247]

Hamer DH, Ward H, Tzipori S, Pereira M, Alroy J, Keusch GT. Attachment of *Cryptosporidium parvum* sporozoites to MDCK cells in vitro. Infection and Immunity 1994;62:2208–2213. [PubMed: 8188342]

Henderson WR Jr, Chi EY. The importance of leukotrienes in mast cell-mediated *Toxoplasma gondii* cytotoxicity. Journal of Infectious Diseases 1998;177:1437–1443. [PubMed: 9593043]

Henderson WR Jr, Rashed M, Yong EC, Fritsche TR, Chiang GK. *Toxoplasma gondii* stimulates the release of 13- and 9-hydroxyoctadecadienoic acids by human platelets. Biochemistry 1992;31:5356–5362. [PubMed: 1606159]

Joe A, Hamer DH, Kelley MA, Pereira MEA, Keusch GT, Tzipori S, Ward HD. Role of a Gal/GalNac-specific lectin in *Cryptosporidiuim parvum*-host cell interaction. Journal Eukaryotic Microbiology 1994;41:44S.

Joe A, Verdon R, Tzipori S, Keusch GT, Ward HD. Attachment of *Cryptosporidium parvum* sporozoites to human intestinal epithelial cells. Infection and Immunity 1998;66:3429–3432. [PubMed: 9632617]

Kelly P, Jack DL, Naeem A, Mandanda B, Pollock RCG, Klein NJ, Turner MW, Farthing MJG. Mannose-binding lectin is a component of innate mucosal defense against *Cryptosporidium parvum* in AIDS. Gastroenterology 2000;119:1236–1242. [PubMed: 11054381]

Langer RC, Schaeffer DA, Riggs MW. Characterization of intestinal epithelial cell receptor recognized by the *Cryptosporidium parvum* sporozoite ligand CSL. Infection and Immunity 2001;69:1661–1670. [PubMed: 11179341]

Lawton P, Naciri M, Mancassola R, Petavy AF. In vitro cultivation of *Cryptosporidium parvum* in the non-adherent human monocytic THP-1 cell line. Journal of Eukaryotic Microbiology 1997;44:66S. [PubMed: 9508448]

Lumb R, Smith K, O'Donaghue PJ, Lanser JA. Ultrastructure of the attachment of *Cryptosporidium* sporozoites to tissue culture cells. Parasitology Research 1988;74:531. [PubMed: 3194366]

MacKenzie WR, Hosie NJ, Proctor ME, Gradus MS, Blair DE, Kazmierczak JJ, Addiss DG, Fox KR, Rose JB, Davis JP. A massive outbreak in Milwaukee of *Cryptospordium* infection transmitted through the public water supply. New England Journal of Medicine 1994;331:161–167. [PubMed: 7818640]

Petersen C, Barnes DA, Gousset L. *Cryptosporidium parvum* GP900, a unique invasion protein. Journal of Eukaryotic Microbiology 1997;44:89S–90S. [PubMed: 9508468]

Rolsma MD, Gelberg HB, Kuhlenschmidt MS. An assay for evaluation of rotavirus cell interactions: Identification of an enterocyte ganglioside fraction that mediates group A procine rotavirus recognition. Journal of Virology 1994;68:258–268. [PubMed: 8254737]

Rolsma MD, Kuhlenschmidt TB, Gelberg HB, Kuhlenschmidt MS. Structure and function of a ganglioside receptor for porcine rotavirus. Journal of Virology 1998;72:9079–9091. [PubMed: 9765453]

Rose, JB.; Lisle, JT.; LeChevallier, M. Waterborne cryptosporidiosis: Incidence, outbreaks, and treatment strategies. In: Fayer, R., editor. Cryptosporidium and cryptosporidiosis. CRC Press; New York: 1997. p. 93-109.

Scott RE. Plasma membrane vesiculation: A new technique for isolation of plasma membranes. Science 1976;194:743–745. [PubMed: 982044]

Thea DM, Pereira MEA, Kotler D, Sterling CR, Keusch GT. Identification and partial purification of a lectin on the surface of the sporozoite of *Cryptosporidium parvum*. Journal of Parasitology 1992;78:886–893. [PubMed: 1403433]

Thulin JD, Kuhlenschmidt MS, Rolsma MD, Muelbroek J, Current WL, Gelberg HB. An intestinal xenograft model for *Cryptosporidium parvum* infection. Infection and Immunity 1994;62:329–331. [PubMed: 8262647]

Tzipori S, Ward H. Cryptosporidiosis: Biology, pathogenesis and disease. Microbes and Infection 2002;4:1047–1058. [PubMed: 12191655]

Upton SJ, Tilley M, Brilhart DB. Comparative development of *Cryptosporidium parvum* (Apicomplexa) in 11 continuous cell lines. Microbiology Letters 1994;118:233–236.

Wolfson JS, Richter JM, Waldron MA, Weber DJ, McCarthy DM, Hopkins CC. Cryptosporidiosis in immunocompetent patients. New England Journal of Medicine 1985;312:1278. [PubMed: 4039408]

Yong EC, Chi EY, Fritsche TR, Henderson WR Jr. Human platelet-mediated cytotoxicity against Toxoplasma gondii: Role of thromboxane. Journal of Experimental Medicine 1991;173:65–78. [PubMed: 1898664]

Yoshikawa H, Iseki M. Freeze-fracture study of the site of attachment of *Cryptosporidium muris* in gastric glands. Journal of Protozoology 1992;39:539–544. [PubMed: 1387896]

Yu JR, Choi SD, Kim YW. In vitro infection of *Cryptosporidium parvum* to four different cell lines. Korean Journal of Parasitology 2000;38:59–64. [PubMed: 10905066]

Zopf D, Roth S. Oligosaccharide anti-infective agents. Lancet 1996;347:1017–1021. [PubMed: 8606566]

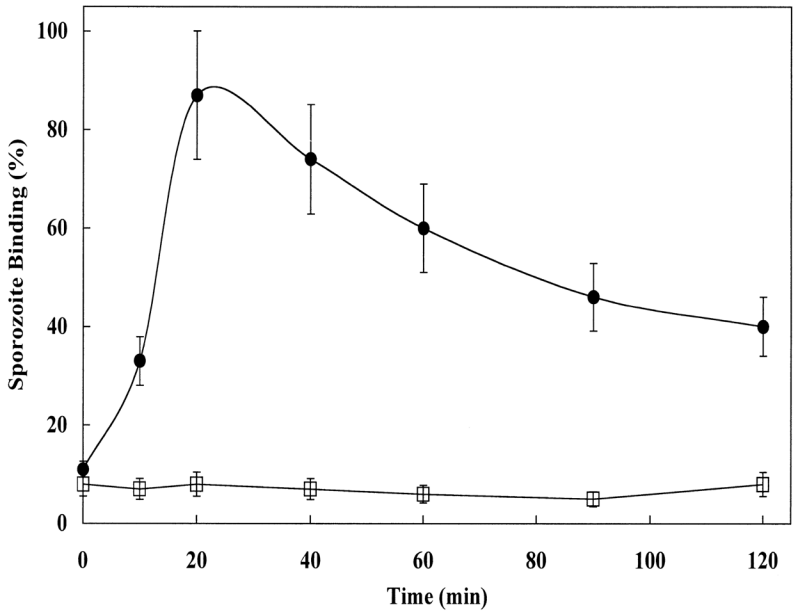

Figure 1.

Kinetics of sporozoite adhesion to MDBK cells. Sporozoites were incubated with MDBK cells and aliquots viewed at the indicated times by phase contrast microscopy to quantify numbers of MDBK cells with attached sporozoites. Sporozoite adhesion is measured as the number of MDBK cells containing at least 1 adhered sporozoite of a total of 100 cells counted (% of MDBK cells bound by sporozoites). *l*: Sporozoites incubated with MDBK cells at 37 C. Note: numerous MDBK cells contain more than 1 bound sporozoite (see Fig. 2). □: Sporozoites incubated with MDBK cells at 4 C.

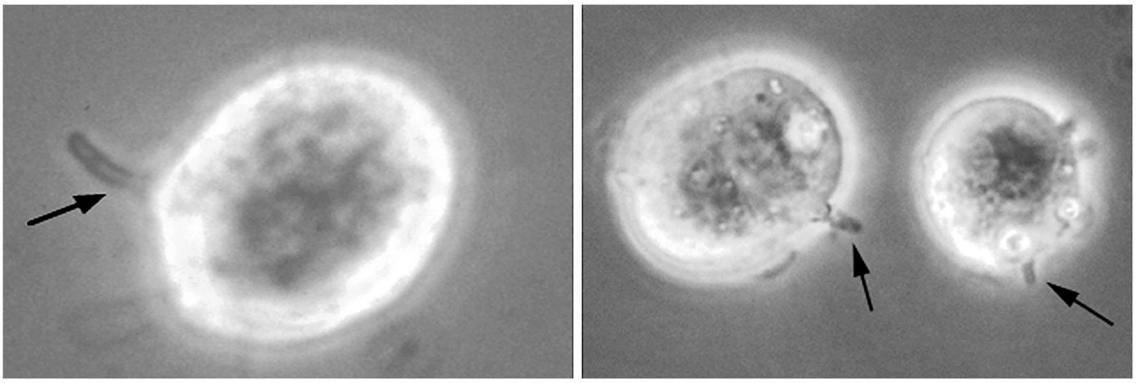

Figure 2.
Phase contrast microscopy of sporozoite binding to MDBK cells. *Cryptosporidium parvum* sporozoites were incubated with MDBK cells. Left, 5-min incubation. Right, 20-min incubation. Arrows denote bound sporozoites. Note: the rightmost cell in the photograph contains 3 bound sporozoites.

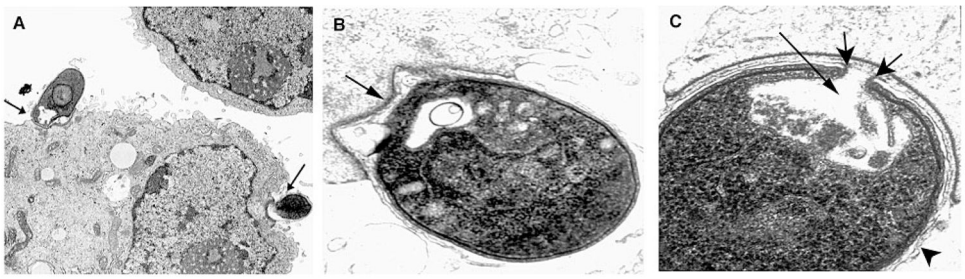

Figure 3.
Transmission electron microscopy of sporozoites adhered to MDBK cells. *Cryptosporidium parvum* sporozoites were incubated with MDBK cells. **A.** Ten-minute incubation (arrows denote bound sporozoites), ×13,200. **B.** Thirty-minute incubation. Note firm adhesion with host cell and beginning development of an electron-dense layer (arrow), ×32,000. **C.** Sixty-minute incubation. Note enlarged anterior invagination (long arrow) and beginning development of an electron-dense collar (short arrows). Also note extension of host plasma membrane surrounding bound sporozoite (arrowhead), ×100,000.

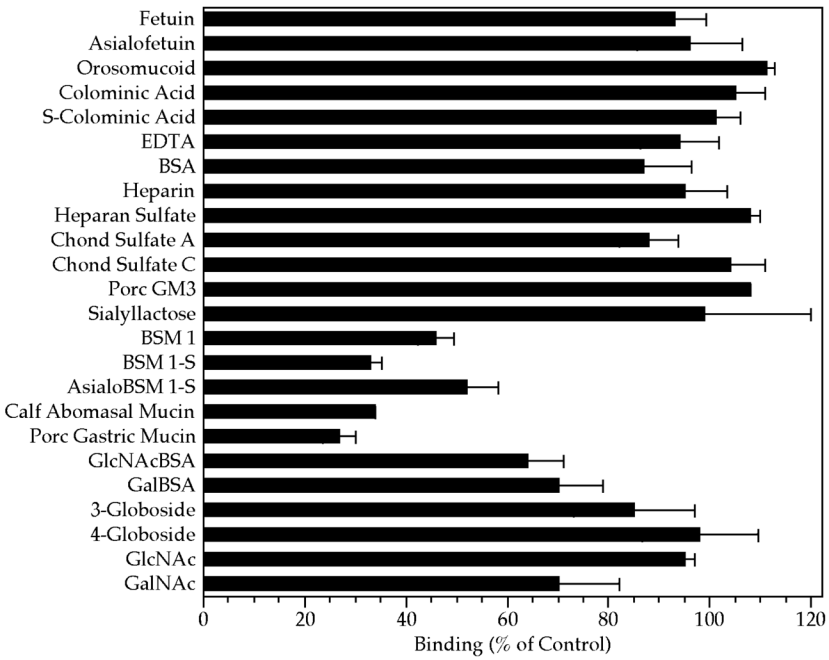

Figure 4.

Effect of various glycoconjugates on sporozoite binding to MDBK cells. Sporozoites and MDBK cells were incubated in suspension at 37 C for 20 min in the absence (control) or presence of the indicated glycoconjugates. After incubation, aliquots of the suspension volumes were examined with phase contrast microscopy. Each glyco-conjugate was compared with separate control incubations, and binding was quantified as the number of sporozoites bound per 100 MDBK cells. All glycoconjugates were added at a final concentration of between 1 and 3 mg/ml, except for the mucins, which were at 0.05 mg/ ml and the neoglycoproteins Gal- and GlcNAc-BSA, which were at 0.2 mg/ml. Monosaccharides were at a final concentration of 2 mM and EDTA was at 10 mM. Key: EDTA, ethylenediamine-tetraacetic acid; BSA, bovine serum albumin; Chond, chondroitin; Porc, porcine; BSM, bovine submaxillary mucin; GlcNAc, *N*-acetyl glucosamine; GalNAc, *N*-acetyl galactosamine.

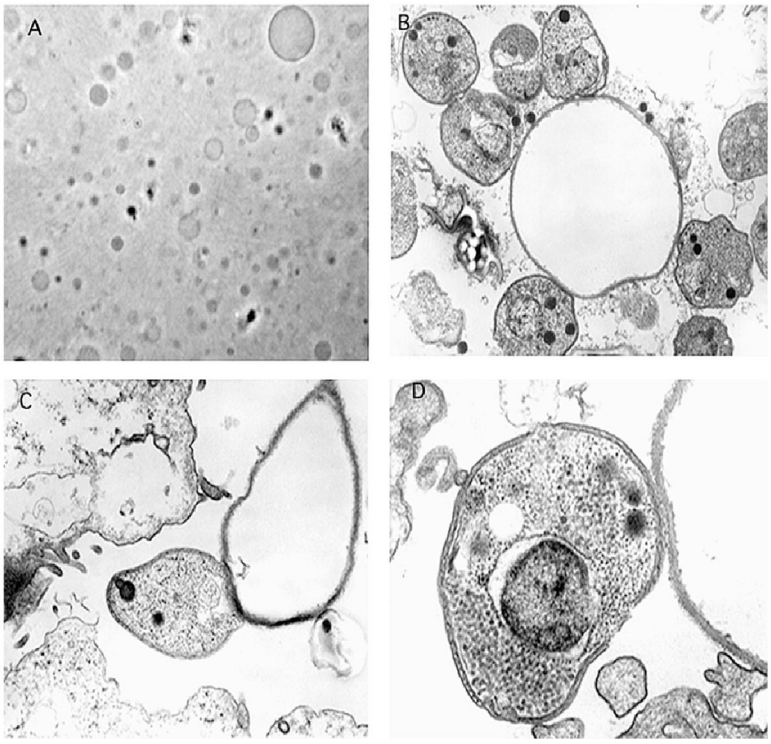

Figure 5.

Phase contrast microscopy of PMVs and transmission electron microscopy of sporozoites adhered to PMVs. **A.** PMVs were generated and examined by phase contrast microscopy. **B.** Sporozoites, MDBK cells, and PMVs were incubated in suspension at 37 C for 20 min. Note single PMV surrounded by several sporozoites, ×20,000. **C.** Note apparent firm adhesion between sporozoite and PMV and possible beginning of sporozoite anterior invagination, ×34,000. **D.** Note apparent weak adhesion between sporozoite and PMV but absence of formation of an electron-dense layer, sporozoite anterior invagination, or parasitophorous vacuole, ×60,000.

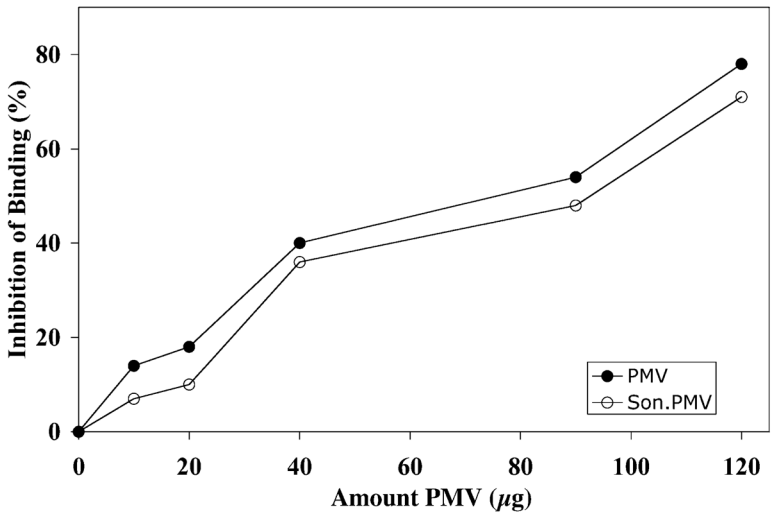

Figure 6.

Effect of PMVs and sonicated PMVs on sporozoite binding to MDBK cells. Sporozoites and MDBK cells were incubated in suspension in the absence (control) and presence of varying amounts of PMVs or sonicated PMVs. After incubation, aliquots of the suspension volumes were examined with phase contrast microscopy. Binding of sporozoites to host cells was quantified as the number of binding events per 100 cells. Note: 50 μg PMV corresponds to 1 × 10^5 MDBK cell equivalents.

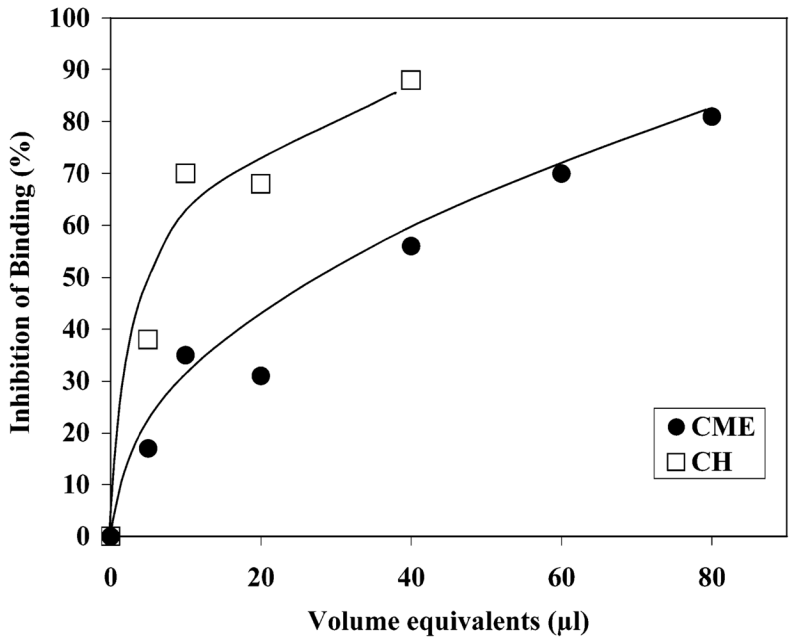

Figure 7.

Effect of organic solvent extracts of MDBK cells on sporozoite binding to MDBK cells. Organic solvent extracts of MDBK cells were generated. *Cryptosporidium parvum* sporozoites and MDBK cells were incubated in suspension at 37 C for 20 min in the absence (control) or presence of varying amounts of the extracts. After incubation, aliquots of the suspension volumes were examined with phase contrast microscopy. Binding of sporozoites to host cells was quantified as the number of binding events per 100 cells. Data are shown as percent inhibition compared with control binding (absence of inhibitors) and compares the sporozoite-binding inhibitory activity of a chloroform: methanol:water extract (CME) of MDBK cells (●) to aliquots of a crude aqueous homogenate (CH) prepared using an equivalent mass of MDBK cells (□).

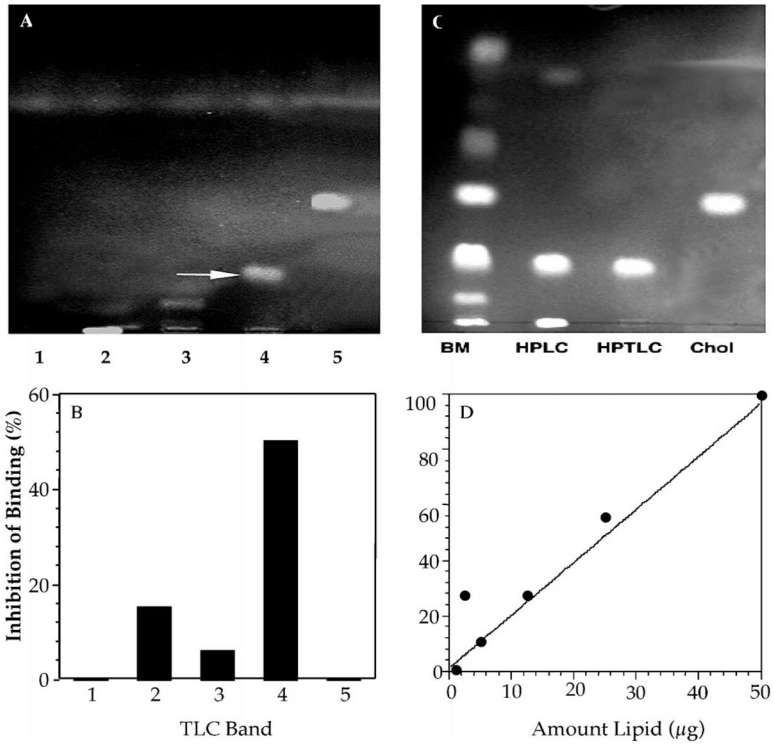

Figure 8.

Purification of sporozoite-binding inhibitory component in bovine mucosa. Organic solvent extracts of bovine mucosa were separated by HPLC and active fractions chromatographed on TLC plates using chloroform:methanol (30:1) as the solvent. Individual bands were scraped from the plates and eluted with chloroform:methanol:water (30:60:20), evaluated for purity and sporozoite-binding inhibitory activity. **A.** Aliquots of the eluate rechromatographed on analytical TLC plates. **B.** Aliquots of each eluted TLC band from the plate shown in panel A were tested for inhibitory activity in the standard binding assay (note band 4 contained the majority of the inhibitory activity). **C.** Band 4 rechromatographed on analytical HPTLC plates developed in chloroform:methanol (30:1) and compared with the starting bovine mucosal extract (BM), active HPLC fraction (HPLC), HPTLC purified band 4 (HPTLC), and cholesterol standard (Chol). Negative controls: areas of each lane, where no stained band was apparent, as well as entire blank lanes and cholesterol bands were scraped, extracted, and tested in the sporozoite-binding assay. None of this fraction exhibited sporozoite-binding inhibitory activity. **D.** Effect of increasing amounts (μg) of purified band 4 on inhibition of sporozoite binding.

Table I

Physical–chemical characteristic of purified sporozoite-binding inhibitor.*

TLC staining characteristics	Result
Primulin (general lipid stain)	Positive
Orcinol (carbohydrate)	Negative
Orcinol ferric chloride (carbohydrates)	Negative
Resorcinol (sialic acid)	Negative
Antimony trichloride (steroid glycoside)	Negative
Phosphorous spray (phosphorus)	Negative
Molybdenum blue (phosphorus)	Negative
Fluorescamine (primary amines)	Negative
Physical–chemical treatments	Effect
Heat (100 C, 15 min)	None
Periodate (10 mM $NaIO_4$, pH 4.5, dark)	None
Base hydrolysis (saponification)	None
Ceramide glycanase	None
Dialysis (10,000 MWCO)	Nondialyzable
Physical–chemical analyses	Result
Mass spectroscopy (FAB)	M + H = 459
Elemental analysis (excluding O)	only C and H detected

* Physical–chemical analyses of the sporozoite-binding inhibitor. The inhibitor (band 4 from Fig. 9) was purified from bovine mucosal extracts and analyzed for TLC staining profiles and chemical and physical characteristics as described in Materials and Methods.